Development of a 2D Vibration Stage for Vibration-assisted Micro-milling

Shaoke WAN [1,2], Naresh Kumar MAROJU [2], Xiaoliang JIN[2]*

(1. *Key Laboratory of Education Ministry for Modern Design & Rotor-Bearing System, Xi'an Jiaotong University, Xi'an, 710049, China;*

2. *Department of Mechanical Engineering, University of British Columbia, BC, Canada, V6T 1Z4)*

* *Corresponding author, email: xjin@mech.ubc.ca, phone:* 604 827 3541

Abstract: Vibration-assisted machining (VAM) has the advantages of extending tool life, reducing cutting force and improving the surface finish. Implementation of vibration assistance with high frequency and amplitude is still a challenge, especially for a micro-milling process. In this paper, a new 2D vibration stage for vibration-assisted micro-milling is developed. The kinematics of the milling process with vibration assistance is modeled, and the effects of vibration parameters on the periodic tool-workpiece separation (TWS) is analyzed. The structure of the vibration stage is designed with flexure hinges, and two piezoelectric actuators are used to drive the stage in two directions. An amplifier is integrated into the vibration stage, and the dynamics of the whole vibration system are identified and analyzed. Micro-milling experiments are conducted to determine the effects of vibration assistance on cutting force and surface quality.

Key words: Micro-milling, Vibration-assisted machining, Piezoelectric actuators, Vibration stage, Tool-workpiece separation.

1 Introduction

With the increasing demand for high-precision components in various industries such as aerospace and communications, continuous efforts have gone to improving the machining performance for production. Vibration-assisted machining (VAM) is a technique in which external vibration at certain amplitude and frequency is superimposed to the original cutting motion in order to extend tool life, reduce the cutting force, and improve the surface quality [1]. To better utilize this technology, the implementation of high-frequency and high-amplitude vibration becomes critical in the VAM process.

Various actuation methods have been developed to apply vibration assistance in a machining process, such as drilling [2-3], turning [4-6], and grinding [7]. Sakaguchi [7] designed a grinding spindle installed with an electromagnetic actuator, which can excite the front end of the spindle during the grinding process. Although the amplitude of vibration can reach up to 10 mm, the maximum frequency is only 200 Hz due to the limitations of the electromagnetic actuator. Meanwhile, a large amount of heat caused by the eddy current loss is generated in the operation, and a cooling system is needed. In order to achieve vibration assistance in higher frequency ranges, both magnetostrictive actuator and piezoelectric actuator have been utilized. Xiang [8] developed a vibration system with a magnetostrictive actuator, which can apply longitudinal vibration with frequency 35 kHz and amplitude 15 μm in the milling of SiCp/Al composites. However, a magnetic core is needed to generate an alternating magnetic field to drive the magnetostrictive actuator, and a cooling system is still desired to reduce the heat caused by the eddy current loss. A piezoelectric actuator has the advantages of high precision, fast response, and compact size, and has attracted much attention for the VAM process. Ko [9], and Razfar and Zarchi [10-11] have developed a workpiece holder installed with piezoelectric actuators, which can generate longitudinal vibration. The cutting forces and tool

wear with vibration assistance have been investigated. Ostasevicius [12] integrated the piezoelectric actuator in a standard tool holder to improve the surface finish of difficult-to-cut materials. However, only the longitudinal vibration was generated, and the vibration amplitude was sensitive to the overall length of the tool and the dimensions of the horn installed in the holder. Wang [13] developed a system which could generate ultrasonic longitudinal-torsional vibration in a helical milling process. All the mentioned vibration devices generate longitudinal or longitudinal-torsional vibrations. For the end milling process, the vibration assistance is usually desired in the feed and cross-feed directions. In order to apply vibration assistance for the end milling process, several 2D vibration stages have been reported recently. Li [14] designed a 2D vibration stage for the micro-milling process, and two piezoelectric actuators were used to generate the vibration, and a single flexible four-bar mechanism was utilized to amplify the vibration amplitude. Based on a flexible mechanism driven by piezoelectric actuators, Chen [15] proposed a 2D vibration stage for micro-milling, and 2 kHz vibration frequency with 10 μm amplitude was achieved. Uhlmann [16] developed a prototype of active workpiece holder, which could apply two-directional vibrations, and the maximum frequency and amplitude were 10 kHz and 7.5 μm, respectively. Jin and Xie [17] developed a 2D vibration stage, and two piezoelectric actuators were installed beside the hinge part to generate the desired vibration. The maximum operation frequency was 11 kHz and the stage displacement was amplified by the hinge part in the frequency range of 5-11 kHz.

Most existing 2D vibration stages have limitations on the operation frequency, which is usually less than 12 kHz. In a micro-milling process, the tooth passing frequencies are much higher than those in conventional milling due to the higher spindle speed. Therefore, vibration assistance at higher frequency is desired in order to enhance the performance of a VAM process.

In the present paper, a new 2D vibration stage that is able to generate vibration assistance in the frequency range 9 kHz-17 kHz is developed for a micro-milling process. The effects of vibration assistance on the instantaneous uncut chip thickness in the milling process is investigated, and the mechanism of periodic tool-workpiece separation (TWS) is analyzed. In the design process, flexible flexure hinges are utilized to transfer the vibration generated by the piezoelectric actuator. In order to achieve a steady input for the piezoelectric actuator and ensure safe operation, a dedicated amplifier is fabricated and integrated with the mechanical components. The dynamic characteristics of the developed vibration stage are identified, and milling experiments with and without vibration assistance are performed to determine the effect of vibration assistance on the milling performance.

The rest of the paper is organized as follows. Section 2 presents theprinciple of a vibration-assisted milling process. Mechanical design and system integration of the vibration stage are presented in Sections 3 and 4. Section 5 presents the experimental results. Conclusions are given in Section 6.

2 Vibration-assisted Milling

Fig. 1 shows a schematic diagram of a milling process with vibration assistance. In a vibration-assisted milling process, vibrations at specific amplitude and frequency are superimposed to the original cutting motion. Due to the difficulties of directly actuating vibration on a rotating tool, the vibration is applied to the workpiece. Usually, vibration assistance can be applied either in the feed direction or in the cross-feed direction, or in both directions simultaneously. In Fig. 1, the coordinate system of workpiece is assumed to be fixed, and the tool tip trajectory relative to the workpiece is superimposed with harmonic motion from the vibration assistance. With appropriate vibration parameters, the tool tip in current cutting motion might overlap with the surface left by the previous tool tip path, which means the

cutting tool loses contact with the workpiece, and the intermittent tool-workpiece contact occurs with repeated penetration and retraction influenced by the vibration assistance. Hence, the uncut chip thickness becomes discontinuous even within a single tooth passing period. Therefore, the TWS caused by vibration assistance is one of the primary features of vibration-assisted milling [18].

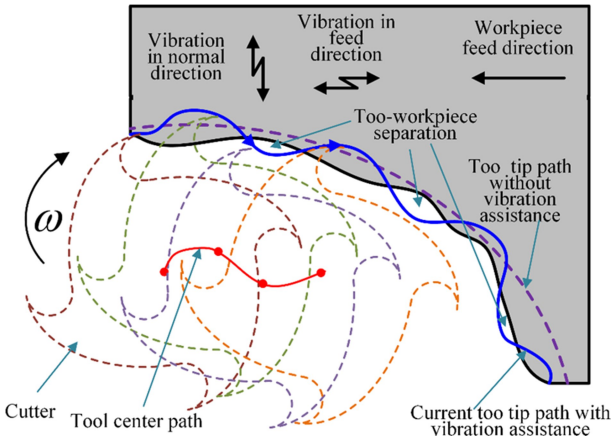

Fig. 1 Schematic diagram of the milling process with vibration assistance.

In order to analyze the effect of vibration assistance on uncut chip thickness, consider the kinematics of the vibration-assisted milling process as illustrated in Fig. 2. XOY is defined as the global stationary coordinate system fixed to the workpiece. The relative feed direction of the tool is defined as the X direction, the cross-feed direction is set as the Y direction. $X_1O_1Y_1$ and $X_2O_2Y_2$ are the tool coordinate system at previous cutting position and current cutting position, respectively, with the origin fixed at the tool center point. The tool coordinate system moves with the tool path relative to the XOY coordinate system. When harmonic vibration is applied to the workpiece, the tool center path relative to XOY is expressed as:

$$\begin{cases} x_0 = ft + a\sin(2\pi f_x + \varphi_x) \\ y_0 = b\sin(2\pi f_y + \varphi_y) \end{cases} \tag{1}$$

where f is the feed rate, a and b are the vibrations amplitudes, f_x and f_y are the vibration frequencies, φ_x and φ_y are the phase angles, in X and Y directions, respectively.

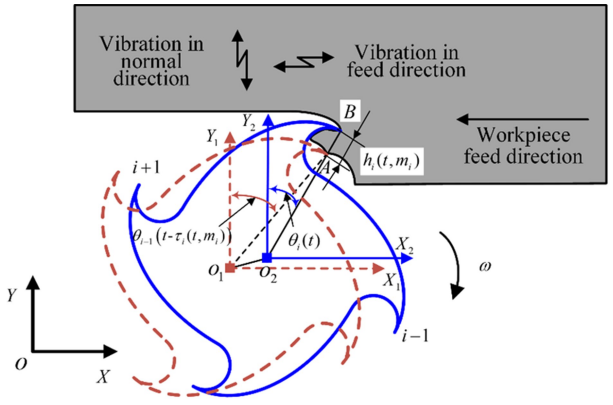

Fig. 2 Kinematics in the vibration-assisted milling process.

As the tool tip might lose contact with the workpiece at some angle position due to the vibration assistance, the instantaneous uncut chip thickness in the current cutting motion might not be generated by the previous tooth. The instantaneous uncut chip thickness $h_i(t,m_i)$ for the i th tooth (shown in Fig. 2) is defined as the distance at point B and point A with the same angle position from previous m_i th tooth ($m_i = 1, 2, \cdots, N$), where N is the number of teeth, and the corresponding time delay between the two cutting motions is denoted by $\tau_i(t,m_i)$. Based on the kinematics of the tool tip considering the vibration assistance, which is shown in Fig.2, the following kinematic equations are obtained:

$$\begin{bmatrix} r\sin(\theta_{i-m_i}(t-\tau_i(t,m_i))) \\ r\cos(\theta_{i-m_i}(t-\tau_i(t,m_i))) \end{bmatrix} = \begin{bmatrix} (r-h_i(t,m_i))\sin(\theta_i(t)) \\ (r-h_i(t,m_i))\cos(\theta_i(t)) \end{bmatrix} + \begin{bmatrix} \tau_i(t,m_i)f + a[\sin(2\pi f_x t + \phi_x) - \sin(2\pi f_x(t-\tau_i(t,m_i)) + \phi_x] \\ b[\sin(2\pi f_y t + \phi_y) - \sin(2\pi f_y(t-\tau_i(t,m_i)) + \phi_y] \end{bmatrix} \tag{2}$$

Based on the kinematic equations, the instantaneous uncut chip thickness in the VAM process is simulated. The rotating speed is 12,000 rpm, and a cutter with 1 mm diameter and 2 flute is used. The

amplitude of vibration is set as 4 μm at a 5 μm/tooth feed rate. The applied vibration frequency is scaled in the ratio $R_f = f_{x/y}/f_s$, where f_s is the spindle rotation frequency. Fig. 3 shows the instantaneous uncut chip thickness when vibration assistance is applied in feed and cross-feed directions. The simulation results show that with the same amplitude and frequency of vibration, the effects of vibration assistance at different directions on the instantaneous uncut chip thickness are different, and TWS occurs more frequently when the vibration assistance is applied in the feed direction. Meanwhile, with a higher frequency of vibration in the feed and cross-feed direction, TWS also occurs more frequently, which illustrates that a higher frequency is desired for the vibration stage.

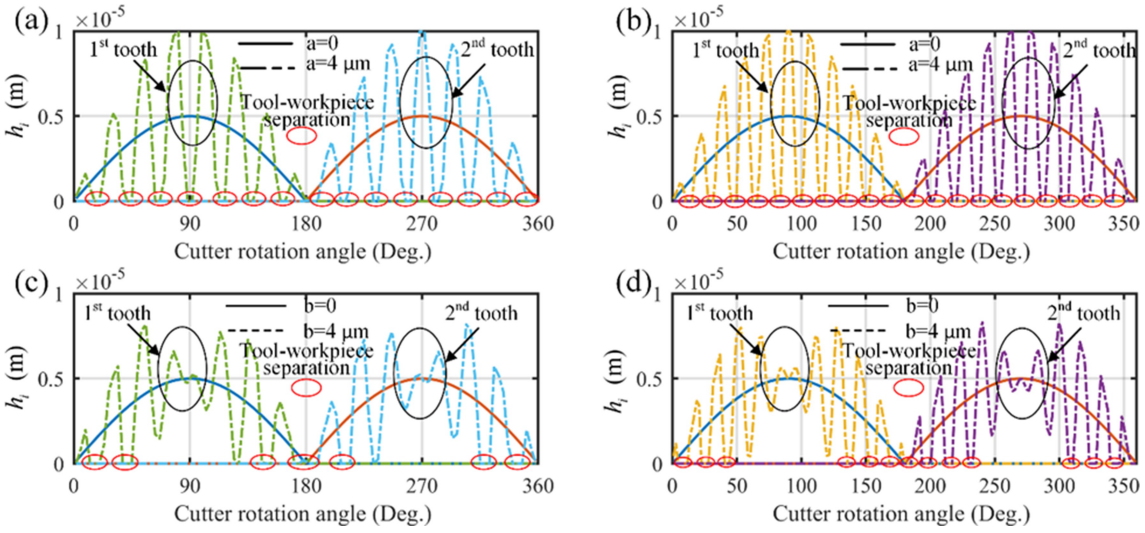

Fig. 3 Instantaneous uncut chip thickness with different vibration conditions: (a) $R_f = 15$, feed direction; (b) $R_f = 21$, feed direction; (c) $R_f = 15$, cross-feed direction; (d) $R_f = 21$, cross-feed direction.

3 Mechanical Design of Vibration Stage

In a micro-milling process, due to the small size and mass of the workpiece, it is feasible to apply the assisted vibration on the workpiece using a vibration stage. Fig. 4 shows a schematic diagram of the designed 2D vibration stage, with two piezoelectric actuators used to generate vibrations in two directions. In each direction, the piezoelectric actuator is preloaded by a bolt and mass block. Due to the advantages of the absence of mechanical friction and high motion sensitivity, a circular flexure hinge is implemented to transmit the motion of the piezoelectric actuator to the center location, where the workpiece is fixed. There are three layers of flexure hinges in each direction to guide the vibration. Meanwhile, the vibration stage takes a symmetrical layout to reduce the cross-coupling effect. In each direction, the structure of the designed vibration stage can be equivalent to a triple four connecting rod flexible mechanism, which is shown in Fig. 5(a). As shown in Fig. 5(b), there are mainly two functional motions for a circular flexure hinge: the rotation around the z-axis and the stretch along the x-axis. As shown in Fig. 5(a), the rotation stiffness of the circular flexure hinge mainly influences the motion of the designed vibration stage in each direction. The rotation stiffness and the stretch stiffness are determined with the dimensions of the circular flexure hinge, which is expressed as [15]:

$$K_\theta = \frac{Ebr^2}{12\left[\dfrac{2s^3(6s^2+4s+1)}{(2s+1)(4s+1)^2} + \dfrac{12s^4(2s+1)}{(4s+1)^{5/2}}\tan^{-1}\sqrt{4s+1}\right]} \tag{3}$$

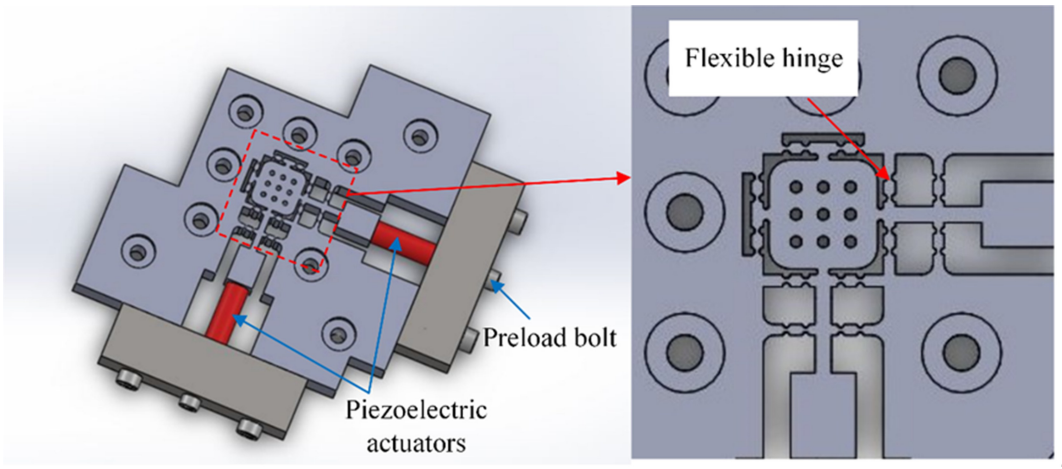

Fig. 4 Schematic representation of the designed 2D vibration stage.

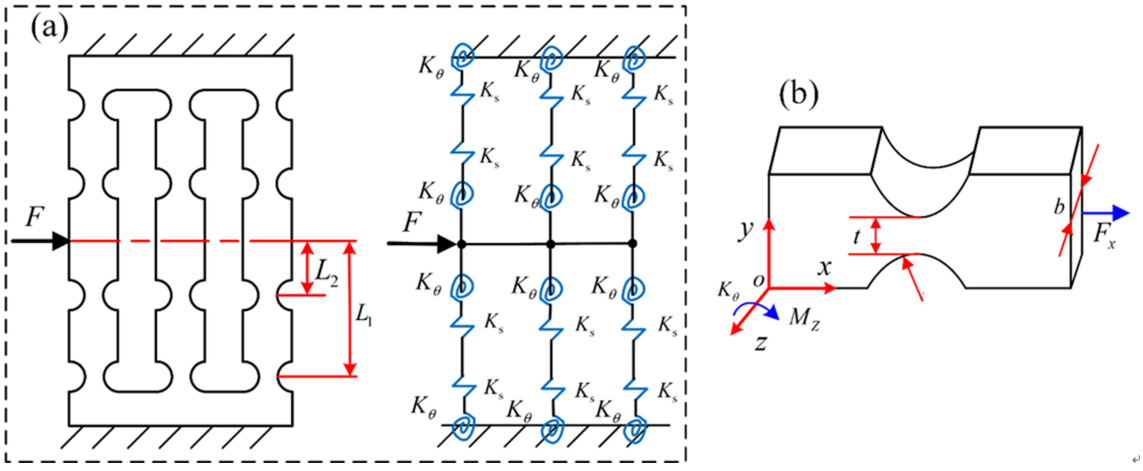

Fig. 5 (a) diagram of a triple four connecting flexible mechanism; (b) schematic diagram of a circular flexure hinge.

$$K_s = \frac{Eb}{\left[\frac{2(2s+1)}{\sqrt{4s+1}}\tan^{-1}\sqrt{4s+1} - \frac{\pi}{2}\right]}$$

where E is the elastic modulus of the material of the flexure hinge, $s = r/t$, and b, r, r are the structural parameters shown in Fig. 5(b).

When the loading force F is applied in the direction as shown in Fig. 5(a), and assuming that the triple four connecting rod flexible mechanism produces a displacement Δs, the power generated by the loading force is expressed as:

$$W = \frac{1}{2}F\Delta s$$

For each circular flexure hinge, the stored energy is

$$W_\theta = \frac{1}{2}K_\theta\theta^2$$

and the rotationangle is expressed as:

$$\theta = \frac{\Delta s}{L_1 - L_2}$$

Assume that all the energy stored by the circular flexure hinges is equal to the power generated by the loading force, the stiffness of the triple four connecting rod flexible mechanism may be expressed the following expression:

$$K_h = \frac{F}{\Delta s} = \frac{12K_\theta}{(L_1 - L_2)^2}$$

Assume that the stiffness of piezoelectric actuator is K_p. Then, the relationship between the displacements of the vibration stage and the piezoelec-

tric actuator is expressed as

$$\Delta L_0 = \Delta L \frac{K_p}{K_p + K_h}$$

where ΔL and ΔL_0 are the motions of the piezoelectric actuator and the stage, respectively, and K_p is the stiffness of the piezoelectric actuator.

Table 1 presents the key parameters of the designed flexible mechanism. The material of the designed vibration stage is 7075 and its elastic modulus is 71 GPa. With Eq. (8), the stiffness of the designed flexible mechanism in each direction is computed as 46 N/μm.

Table 1 Parameters of the designed flexible mechanism.

Parameters	b	r	t	L_1	L_2
Value (mm)	17	0.725	0.8	6.775	3.225

Considering the mounting dimensions and operation stiffness, two Physik Instrument piezoelectric actuators (model: P-010.20H) are selected to drive the vibration stage. Their specifications are given in Table 2. With Eq. (9) and the parameters of the selected piezoelectric actuator, the maximum displacement which the stage can achieve is determined as 17 μm.

Table 2 Specifications of P-010.20H piezoelectric actuator.

Travel range	30μm	Frequency	39 KHz
Length	27mm	Capacitance	82 nF
Force	1800N	Operating voltage	0~1000V
Stiffness	59N/μm	Outside diameter	10 mm

4 System Integration of Vibration Stage

As mentioned in Section 2, a higher frequency of the vibration stage is desired to ensure frequent occurrence of the TWS. Furthermore, the amplitude of vibration should be in the same order as the feed rate in order to ensure the effectiveness of the vibration assistance. Therefore, the voltage and current should be sufficient to drive the piezo-actuator within a large bandwidth. However, it has always been a challenge to design a circuit to drive the piezoelectric actuator steadily and safely, and the selection of a suitable amplifier is especially important in this context.

Usually, the piezoelectric actuator is equivalent to a capacitive load, which is 82 nF in the designed vibration stage. The maximum vibration frequency that is expected to achieve is 20 kHz. In this paper, first the desired operation voltage with a peak-to-peak value 200 V is set up. For amplifiers, the limitations in slew rate capability, which defines the ability of tracking the changes in output, might lead to nonlinear effects. The slew rate should satisfy the following relationship:

$$SR \geq 2\pi f V_{peak}$$

where f is the operating frequency, and V_{peak} is the peak amplitude of the output voltage. Based on the frequency and the voltage for the developed vibration stage, the slew rate of the amplifier should be larger than 12.6 V/μs.

The capacitive reactance of the piezoelectric actuator at the maximum operating frequency is expressed as:

$$X_c = \frac{1}{2\pi f C}$$

where f and C are operation frequency and equivalent capacitance, respectively. The maximum power dissipation by the piezoelectric actuator is calculated using the equation

$$P = \frac{V_{p\text{-}p}^2}{2\pi X_c}$$

and the maximum powerof amplifier should be larger than 65.6 W.

Unfortunately, it is found that most of the commercially available amplifiers for piezoelectric actuator cannot satisfy these requirements simultaneously. In this paper, a power operational amplifier module (MP118FD, Apex Micro-technology) and the evaluation kit EK57 are selected to build an amplifier that can operate the selected piezoelectric actuator. The maximum amplitude of the output voltage and the output power are 100 V and 100 W, respectively, and its SR is 80 V/μs. Hence, its maximum op-

erating frequency can satisfy the requirement.

Fig. 6 shows the schematic diagram of the amplifier built in the designed vibration stage system. R_i and R_f are the input resistance and the feedback resistance, respectively, which determine the gain of the amplifier. In this design, 9.7 kΩ and 475 Ω are chosen for these resistances, to realize a gain of about 20. It should be noted that the piezoelectric actuator might generate a reverse voltage due to its deformation during vibration process, and the diode should be used to prevent the reverse voltage from reaching the amplifier. Two SUR1560 ultra fast rectifier diodes are selected and their connections are shown in Fig. 6 (annotated by D_1 and D_2, respectively). For the stability of the overall system, an isolation resistor, with resistance R_s (see Fig. 6) is connected between the output of the amplifier and the piezoelectric actuator. The resistance R_s is selected with the crossover frequency analysis of the RC circuit (constructed by the piezoelectric actuator and the isolation resistor). In the design, a crossover frequency value greater than 1 MHz is chosen to make sure that the phase margin at 20 kHz for the whole circuit (output of amplifier and RC circuit) is greater than or equal to 60°. Therefore, the RC circuit should satisfy the condition that $1/R_sC>1MHz$ and the resistance R_s should be less than 12 Ω. Then an isolation resistor of resistance 7.5 Ω (model TO220, Ohmite) is selected in the design.

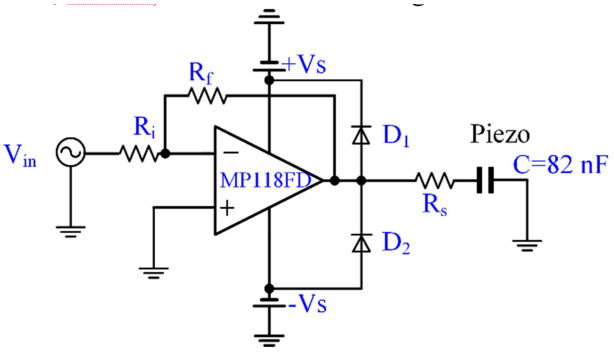

Fig. 6 Circuit diagram of the amplifier.

Fig 7 shows the final schematic diagram of the overall vibration stage system. The amplifier is driven by two high-voltage DC power supplies, which are utilized to offer the positive and negative DC output, respectively. Signal generator provides the input control voltage signal to the amplifier. The input voltage is amplified with a gain of 20, and the amplified voltage drives the piezoelectric actuator to produce motion in the workpiece. The system is driven in each direction by one piezo-actuator.

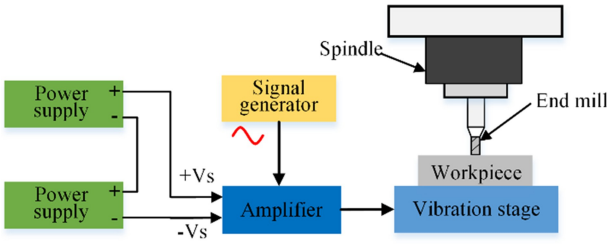

Fig. 7 Schematic diagram of the vibration stage and the machining process.

5 Experiments

In this section, the dynamic performance of the designed vibration stage system is examined. The achievable amplitude of vibration at different frequencies is measured. Based on the analysis of the TWS in the vibration-assisted milling process in Section 2, micro-milling experiments with and without vibration assistance are performed to investigate the effects of vibration on the surface quality.

5.1 Identification of Vibration Stage Dynamics

Fig. 8 shows the setup for the test of the designed vibration stage. Two high-voltage power supplies are connected in series to provide ±100 V voltage, and a signal generator is used to provide a sinusoidal input signal for the amplifier. A laser Doppler vibrometer is utilized to measure the vibration of the workpiece fixed on the vibration stage, and a National Instruments general-purpose data acquisition system (DAQ) is used to record the vibration signals.

A sweep test is performed to measure the maximum achievable amplitude of the vibration stage at different frequencies. A sinusoidal signal with an amplitude of 8.5 V (peak to peak) is generated and

provided to the amplifier. The frequency varies from 1 kHz to 20 kHz within 10 s, and a linear sweep mode is utilized. Fig. 9(a) shows the vibration response in the time domain. It can be found that several peaks emerge, and the maximum amplitude is about 10 μm (peak to peak). Fig. 9(b) illustrates the spectrum of the measured vibration response, and the two frequencies with the largest vibration amplitude are 9,210 Hz and 10,050 Hz, respectively. At 16,920 Hz, the corresponding peak-to-peak amplitude is about 4 μm. It should be noted that a conservative amplified voltage of 170 V (peak to peak) is chosen in the test. Although the amplitude at 16,920 Hz is only about 4 μm (peak to peak) in the test results, the amplitude can achieve a higher magnitude when a higher operation voltage is applied to the piezoelectric actuator. In order to increase the available operation voltage, two amplifiers will be bridged together in the future, which could achieve an operation voltage close to 400 V (peak to peak).

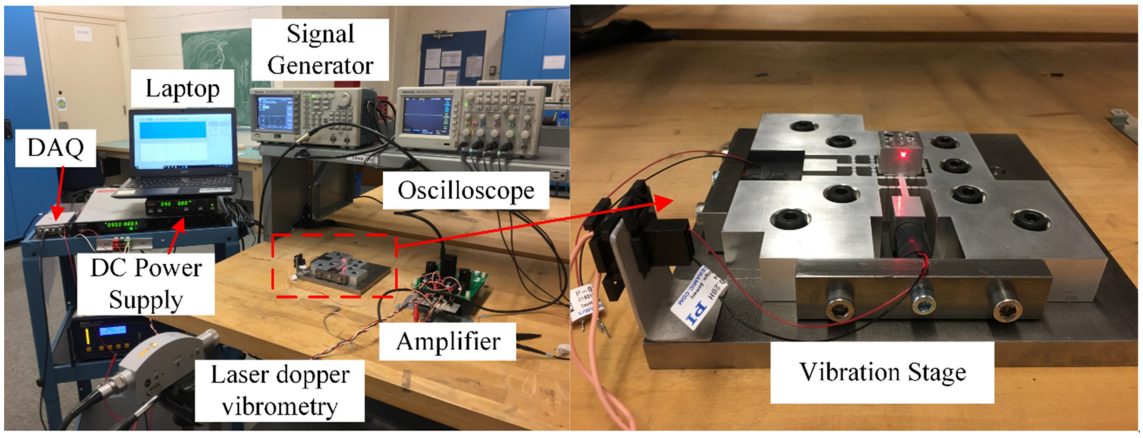

Fig. 8 Experimental setup to test the vibration stage.

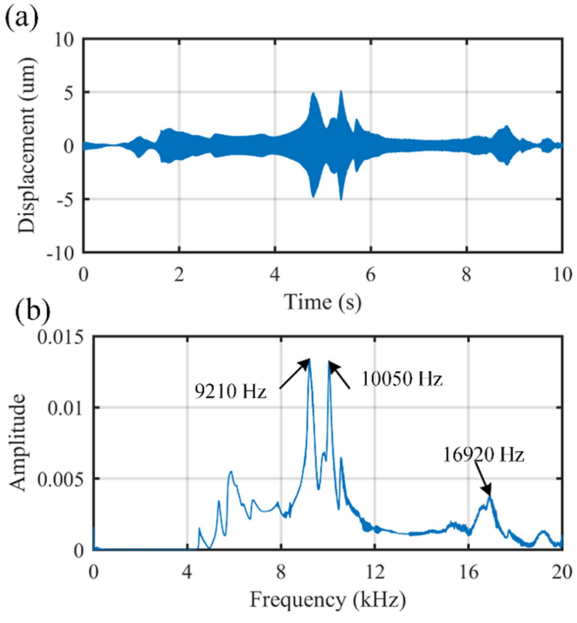

Fig. 9 (a) sweep search, and (b) vibration modes of the vibration stage.

5.2 Micro-milling Experiments with Vibration Assistance

Milling experiments are performed on a micro-milling machine (shown in Fig. 10) to determine the actual cutting performance with vibration assistance. The developed vibration stage is fixed on a dynamometer, which is mounted on the machine stage. In the milling experiment, the spindle speed is set at 40,000 rpm, and the frequency of vibration assistance is 10.1 kHz, which is almost 15 times of the rotating frequency of the spindle. The amplitude (peak to peak) of the control signal is set at 8.5 V, which is expected to achieve a vibration amplitude of 5 μm. An end mill with 1 mm diameter and 2 flutes is chosen. The workpiece material is aluminum alloy 7075. The other cutting parameters are: feed rate = 5 μm/tooth, radial and axial cutting depths are 0.2 mm and 1 mm, respectively.

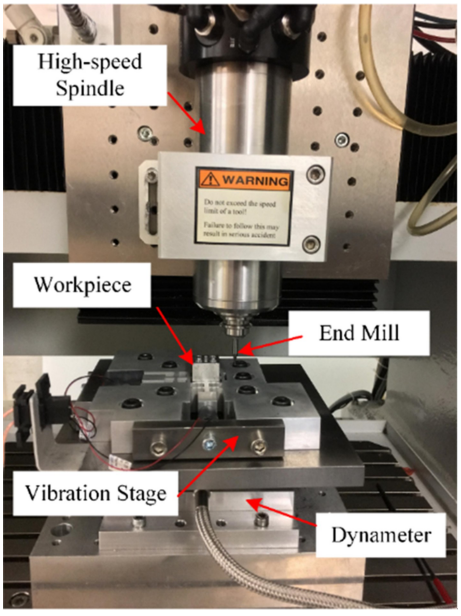

Fig. 10 Experimental setup of vibration-assisted micro-milling.

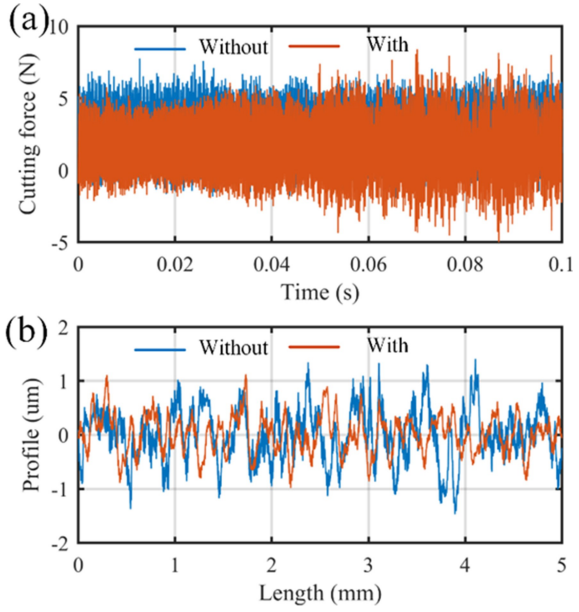

Fig. 11 (a) Cutting force (b) surface profiles with and without vibration.

The milling experiments with and without vibration assistance are conducted, and Fig. 11 shows theresulting measured cutting force and surface profiles. From Fig. 11(a) it is seen that the maximum cutting force with vibration is smaller than the condition without vibration, and the decrease is about 20%. The profile shown in Fig. 11(b) also illustrates an improvement of surface quality, and the surface roughness improves from $Ra = 0.35$ to $Ra = 0.23$. The results show that the vibration assistance applied by the developed stage can improve the milling process, effectively.

6 Conclusions

In this paper, a vibration assistance system was developed for implementing vibration assistance in a micro-milling process. Through a kinematic analysis, it was found that the vibration assistance resulted in the change of instantaneous uncut chip thickness and the occurrence of TWS. In order to obtain an effective vibration assistance with required amplitude and frequency, piezoelectric actuator was chosen to excite a stage composed with a series of flexure hinges. A low-cost amplifier was built to drive the piezoelectric actuator. The maximum amplitude of the vibration stage is about 10 μm (peak to peak), and two frequencies with the largest amplitude at 9,210 Hz and 10,050 Hz were achieved. Though the amplitude at 16,920 Hz was only about 4 μm (peak to peak), the amplitude is expected to be higher by bridging the two amplifiers, and this work will be performed in a future study. Micro-milling experiment with vibration assistance showed an improvement of the cutting performance in reducing the cutting force and the surface roughness. The effect of vibration assistance on milling dynamics will be investigated in a future study.

ACKNOWLEDGMENT

This research is supported by NSERC – Discovery FundsRGPIN-2018-04911, and is partly supported by China Scholarship Council.

References

[1] Kumar, M. N., Subbu, S. K., Krishna, P. V., & Venugopal, A. (2014). Vibration assisted conventional and advanced machining: A review. Procedia Engineering, 97, 1577-1586.

[2] Liao, Y. S., Chen, Y. C., & Lin, H. M. (2007). Feasibility study of the ultrasonic vibration assisted drilling of Inconel superalloy. International Journal of Machine Tools and Manufacture, 47(12-13), 1988-1996.

[3] Chang, S. S., & Bone, G. M. (2010). Burr height model for vibration assisted drilling of aluminum 6061-T6. Precision Engineering, 34(3), 369-375.

[4] Zhou, M.,Eow, Y. T., Ngoi, B. K. A., & Lim, E. N. (2003). Vibration-assisted precision machining of steel with PCD tools. Materials and Manufacturing Processes, 18(5), 825-834.

[5] Maroju, N. K., Vamsi, K. P., & Xiaoliang, J. (2017). Investigations on feasibility of low frequency vibration-assisted turning. The International Journal of Advanced Manufacturing Technology, 91(9-12), 3775-3788.

[6] Maroju, N. K., Krishna, P. V., & Jin, X. (2017). Assessment of high and low-frequency vibration assisted turning with material hardness. International Journal of Machining and Machinability of Materials, 19(2), 110-135.

[7] Katsumi S, Junichiro K (1975) Impact properties of the ultrasonic vibrating grinding wheel. J Japan Soc Precis Eng 41(485):559 - 564

[8] Xiang, D. H., Yue, G. X.,Zhi, X. T., Gao, G. F., & Zhao, B. (2011). Study on cutting force and tool wear of high volume SiC/Al MMCs with ultrasonic vibration high-speed milling. In Key Engineering Materials (Vol. 455, pp. 264-268). Trans Tech Publications.

[9] Ko, J. H., & Tan, S. W. (2013). Chatter marksreduction in meso-scale milling through ultrasonic vibration assistance parallel to tooling's axis. International Journal of Precision Engineering and Manufacturing, 14(1), 17-22.

[10] Razfar, M. R., Sarvi, P., & Zarchi, M. A. (2011). Experimental investigation of the surface roughness in ultrasonic-assisted milling. Proceedings of the Institution of Mechanical Engineers, Part B: Journal of Engineering Manufacture, 225(9), 1615-1620.

[11] Abootorabi Zarchi, M. M., Razfar, M. R., & Abdullah, A. (2012). Investigation of the effect of cutting speed and vibration amplitude on cutting forces in ultrasonic-assisted milling. Proceedings of the Institution of Mechanical Engineers, Part B: Journal of Engineering Manufacture, 226(7), 1185-1191.

[12] Ostasevicius, V., Gaidys, R., Dauksevicius, R., & Mikuckyte, S. (2013). Study of vibration milling for improving surface finish of difficult-to-cut materials. Journal of Mechanical Engineering, 59(6), 351-359.

[13] Wang PC.(2014) Research on devices in ultrasonic longitudinal-torsional vibration helical milling [D]. Harbin Institute of Technology School of Mechatronics Engineering Master Theses.

[14] Li G.(2012) Non-resonant vibration auxiliary table development and study on micro-milling technology experiment [D]. Harbin institute of technology.

[15] Chen, W., Huo, D., et al. (2017). Design, analysis and testing a high bandwidth XY stage for vibration-assisted milling, Proceedings of the 17th Europen International Conference, Hannove, Germany

[16] Uhlmann, E., Perfilov, I., & Oberschmidt, D. (2015, June). Two-axis Vibration System for Targeted Influencing of Micro-milling. In Proceedings of the European Society for Precision Engineering and Nanotechnology - (EUSPEN): 15th international conference & exhibition of the European Society of Precision Engineering and Nanotechnology (pp. 325-326).

[17] Jin, X., & Xie, B. (2015). Experimental study on surface generation in vibration-assisted micro-milling of glass. The International Journal of Advanced Manufacturing Technology, 81(1-4), 507-512.

[18] Chen, W.,Huo, D., Hale, J., & Ding, H. (2018). Kinematics and tool-workpiece separation analysis of vibrationassisted milling. International Journal of Mechanical Sciences, 136, 169-178.

Authors' Biographies

Shaoke WAN is a Ph. D. student at Xi'an Jiaotong University, China. Currently he is a visiting student at the University of British Columbia, Vancouver, Canada. His research interests are in the dynamics of vibration-assisted milling process, and active control for milling chatter.

E-mail: wanshaoke@163.com

Naresh Kumar MAROJU is a Ph. D. Student in the Department of Mechanical Engineering at the University of British Columbia, Canada. His research direction is surface texturing process and machining of bulk metallic glasses.
E-mail: nareshkm@alumni.ubc.ca

Xiaoliang JIN is an Assistant Professor in the Department of Mechanical Engineering at the University of British Columbia, Canada. His research includes mechanics and dynamics of the micro-cutting process, vibration assisted machining of brittle materials, precision manufacturing processes, and CNC design.
E-mail: xjin@mech.ubc.ca